Biochemical Society Transactions (2024) **52** 491–501
https://doi.org/10.1042/BST20231315

PORTLAND PRESS

Review Article

Folding speeds of helical membrane proteins

Duyoung Min[1,2]

[1]Department of Chemistry, Ulsan National Institute of Science and Technology, Ulsan 44919, Republic of Korea; [2]Center for Wave Energy Materials, Ulsan National Institute of Science and Technology, Ulsan 44919, Republic of Korea

Correspondence: Duyoung Min (dymin@unist.ac.kr)

Membrane proteins play key roles in human health, contributing to cellular signaling, ATP synthesis, immunity, and metabolite transport. Protein folding is the pivotal early step for their proper functioning. Understanding how this class of proteins adopts their native folds could potentially aid in drug design and therapeutic interventions for misfolding diseases. It is an essential piece in the whole puzzle to untangle their kinetic complexities, such as how rapid membrane proteins fold, how their folding speeds are influenced by changing conditions, and what mechanisms are at play. This review explores the folding speed aspect of multipass α-helical membrane proteins, encompassing plausible folding scenarios based on the timing and stability of helix packing interactions, methods for characterizing the folding time scales, relevant folding steps and caveats for interpretation, and potential implications. The review also highlights the recent estimation of the so-called folding speed limit of helical membrane proteins and discusses its consequent impact on the current picture of folding energy landscapes.

Biogenesis of helical membrane proteins

The biogenesis of multipass helical membrane proteins involves four primary steps [1]: (1) the targeting of a nascent polypeptide chain to eukaryotic endoplasmic reticulum (ER) or bacterial plasma membrane, (2) the insertion of the chain into lipid bilayers with an appropriate topology and formation of transmembrane (TM) helices, (3) the folding into the functional tertiary structure mainly through the lateral packing of TM helices, and, (4) if any, the assembly of the tertiary folds into a higher-level complex. The middle two steps are commonly regarded as constituting the core folding process. In the co-translational folding pathway [1–5], the helix insertion is mainly mediated by the Sec translocon complex while being translated from a ribosome bound to the complex (the first-stage folding). The helices then dissociate from the ribosome–translocon complex and associate with each other until adopting the compact native fold (the second-stage folding).

The helix packing interactions may also initiate early on the ribosome–translocon complex [3,4]. Unless there is a strong packing cooperativity across the entire protein, the two folding steps would occur simultaneously along the pathway [2]. This coupling is likely a prominent feature, particularly for large membrane proteins with clearly separated, multiple TM domains [6–9]. The extent of coupling between the two stages and the resulting time scales of the entire folding process will depend on various factors, including the rates of translation and insertion, rate and stability of helix packing interactions, protein size and independence of folding domains, and specific local/global folds like re-entrant helices and knots. Accessory proteins such as insertases and chaperones can participate in the overall folding process as essential components, including those like Oxa1 superfamily insertases and calnexin [1,10]. In this review article, I will focus on simplified *in vitro* folding studies that offer quantitative evaluations of folding speeds of helical membrane proteins.

Received: 9 January 2024
Revised: 7 February 2024
Accepted: 9 February 2024

Version of Record published:
22 February 2024

Plausible folding scenarios of helical membrane proteins

The folding process of helical membrane proteins may manifest in three primary scenarios based on the timing and stability of helix packing interactions (Figure 1). In the sequentially accrued folding,

Biochemical Society Transactions (2024) **52** 491–501
https://doi.org/10.1042/BST20231315

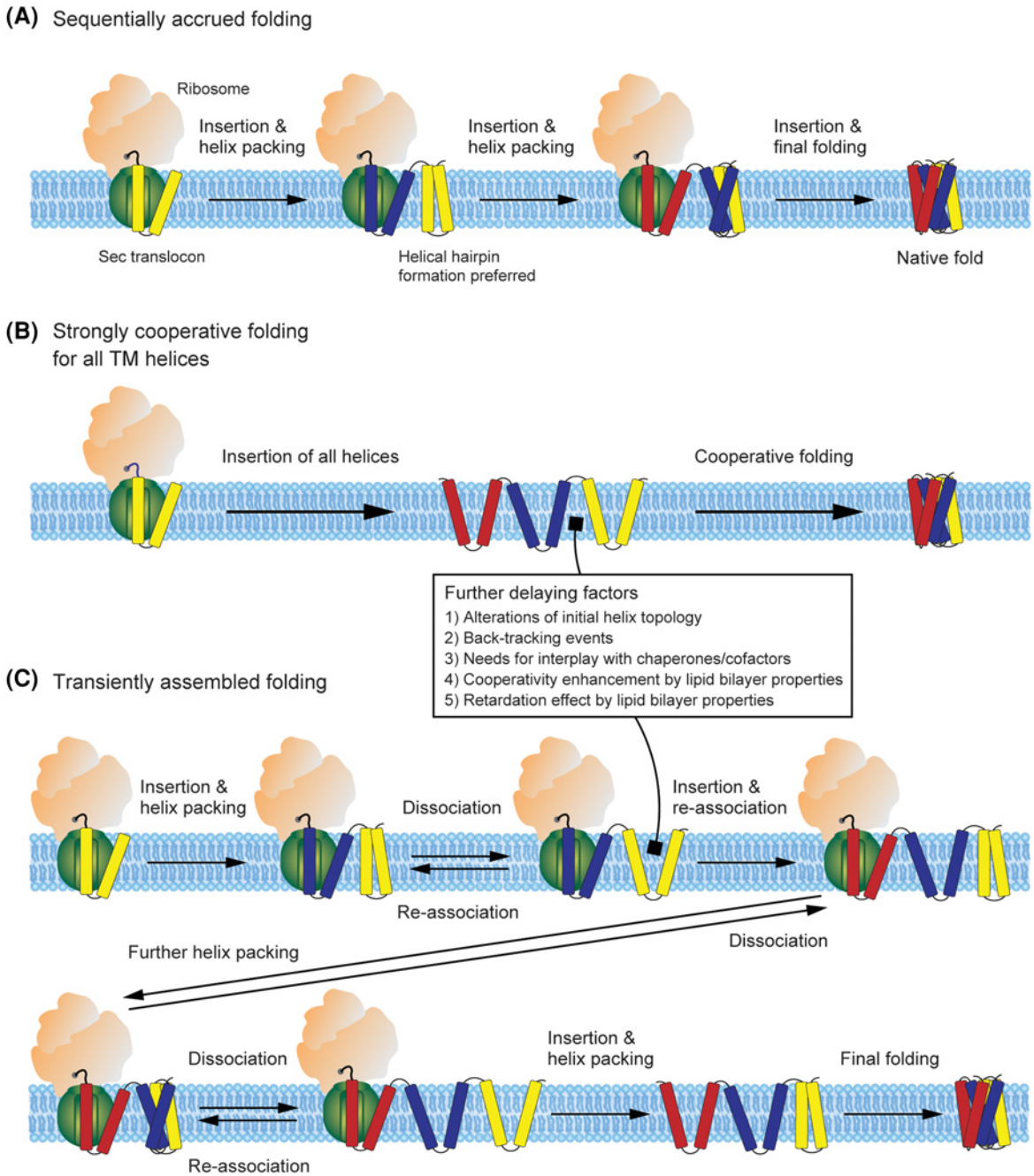

Figure 1. Plausible folding scenarios of helical membrane proteins.

(**A**) Sequentially accrued folding. TM helices accumulate in a stable manner within lipid bilayers during translation and insertion. (**B**) Strongly cooperative folding for all TM helices. The folding transition takes place in a single step after the complete translation and insertion of all helices. (**C**) Transiently assembled folding. TM helices frequently form less stable intermediate structures that rapidly dissociate during translation and insertion until adopting the final stable fold. This folding scenario likely represents a more realistic case compared with the two extreme scenarios shown in (**A**) and (**B**). Lipid bilayers are shown as sky blue.

the inserted TM helices accumulate early and steadily within lipid bilayers, maintaining stable structures throughout the translation and insertion (Figure 1A). For this case, the translation event would serve as a principal limiting factor on overall folding speeds, given the slow elongation of polypeptide chains at 2–17 amino

acids per second (6–50 s for 100 amino acids) [11–18]. The second layer of the folding speed constraint involves the helix insertion into lipid bilayers. The insertion rate is slightly faster than the elongation rate, roughly ranging from 10 to 20 amino acids per second (1–2 s for a TM helix) [3,4,13,19]. The time scale of seconds required for helix insertion is still much slower than a hundred of milliseconds needed for the formation of a helical hairpin, which is a preferred folding unit [2,6,20], and its subsequent packing on the structured template within lipid bilayers [21].

In case of the strongly cooperative folding for all TM helices, the helix packing and folding transition occurs as a single step after the complete translation and insertion of all helices (Figure 1B). In contrast, in a more realistic scenario of the transiently assembled folding, the TM helices frequently form less stable intermediate structures that rapidly dissociate during the translation and insertion until ultimately adopting the final stable fold (Figure 1C). For these folding scenarios, the entire folding times would not be solely limited by the earlier events of translation and insertion, but likely be delayed compared with what is expected for the sequentially accrued folding. The second-stage folding can be further set back by various other factors, such as alterations in initial helix topology [22–27], back-tracking events [28], the need for interplay with chaperone proteins and/or cofactors [1,7,29–31], and the cooperativity enhancement and retardation effect by lipid bilayer properties [32–37].

Previous *in vitro* folding studies offer intriguing insights suggesting that the prevalence of delayed and/or slow second-stage folding may be a characteristic feature in many helical membrane proteins. For instance, a rhomboid protease GlpG mainly comprising six TM helices was shown to undergo cooperative folding from the unfolded helical state [38–40]. The entire folding time for GlpG was notably slower compared with the helical hairpin formations within lipid bilayers, by a factor of 20–30 ([21,39]; see the section *Folding speeds under mechanical unfolding approaches* for more details). Despite its relatively small size with four-TM helices, peripheral myelin protein 22 (PMP22) was observed to undergo remarkably slow folding, taking up to an hour at very low denaturant concentrations [41,42]. This slowness may be attributed to intrinsic slow folding kinetics and/or marginal conformational stability [41,42]. The entire half domain of lactose permease (LacY) can be flipped across the lipid bilayer even after the translation and insertion are completed, taking up to several minutes [25].

These illustrative cases evoke the original two-stage folding model [43,44], where the insertion of helices is followed by their association with clean separation, as a practically useful framework in folding studies despite its simplicity. Several *in vitro* methods have characterized the folding time scales of selected model membrane proteins, with a primary focus on the second-stage folding or spontaneous insertion coupled with helix formation and packing (Figure 2 and Table 1). As detailed methodological reviews can be found elsewhere [6,48–50], only their major features, relevant folding steps, and caveats in interpretations are briefly outlined in the following sections. The cell-free expression approaches employing surface-enhanced infrared absorption spectroscopy (SEIRAS) [29,51] are omitted in this review, as their exceptionally prolonged time scales of several hours may involve stochastic, non-synchronized initiation of protein translation, spontaneous insertion, and structure formation.

Folding speeds under chemical denaturation approaches

In chemical denaturation methods (Figure 2A), membrane proteins in detergent micelles, mixed detergent/lipid micelles, or vesicle bilayers are initially denatured by chemical denaturants like sodium dodecyl sulfate (SDS) or urea [10,52–55]. The denatured proteins with full or partial helical content are then refolded by diluting the denaturant concentration. The observed rate constants at different denaturant concentrations are determined by monitoring the transitions through (un)folding reporters, such as intrinsic fluorescence, protein absorbance, circular dichroism spectra, and pulse proteolysis. These values are extrapolated to zero denaturant concentration. Folding time scales for helical membrane proteins with four to seven TM helices, including disulfide bond formation protein B (DsbB), GlpG, and bacteriorhodopsin (bR), were estimated to fall within the range of 1–10 s in detergent micelles or mixed detergent/lipid micelles [40,45–47] (Table 1). The interpretation of kinetics can sometimes be complicated by a less well-defined, chemically denatured state, especially concerning the locations of unstructured parts and the topology of helices in the reconstituted solvent space. The extrapolation analysis may introduce non-negligible errors in the estimated folding speeds, especially for bR, as it is almost completely folded at low denaturant concentrations, requiring a long extrapolation from high denaturant concentrations [38,56].

Biochemical Society Transactions (2024) **52** 491–501
https://doi.org/10.1042/BST20231315

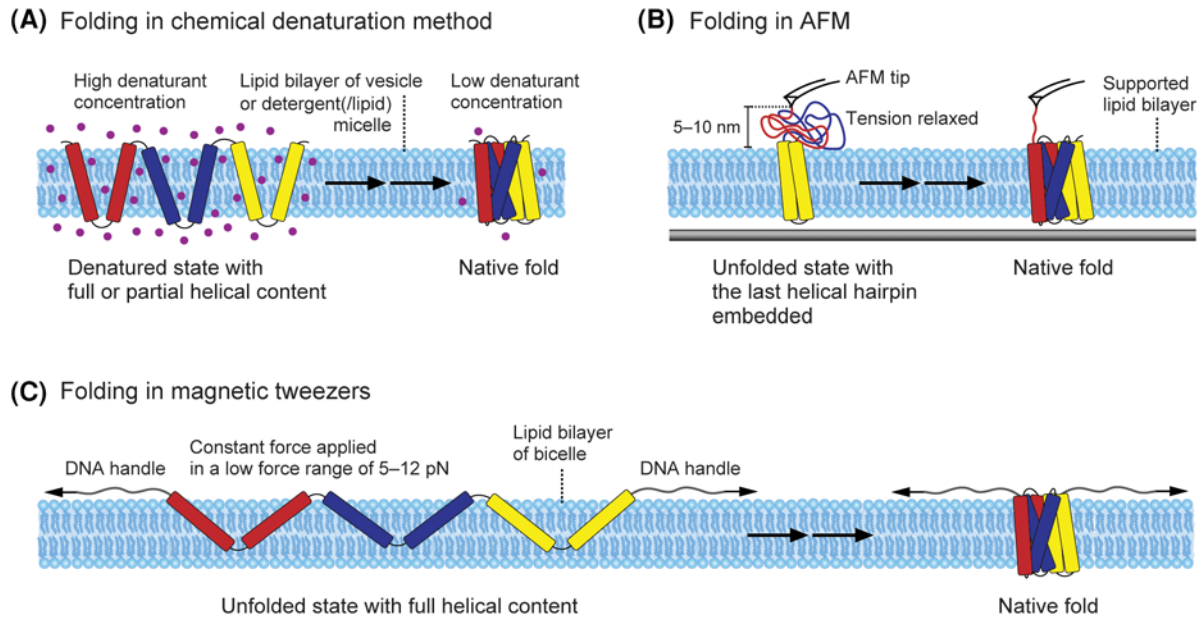

Figure 2. Main methods for characterizing the folding speeds of helical membrane proteins.

(**A**) Chemical denaturation approach. Membrane proteins in vesicle bilayers, detergent micelles, or mixed detergent/lipid micelles are initially denatured using chemical denaturants like SDS or urea (left). The purple dots represent the chemical denaturants. The denatured proteins, with full or partial helical content, are refolded by diluting the denaturant concentration (right). The observed rate constants at different denaturant concentrations are determined by monitoring the transitions and extrapolated to zero denaturant concentration. (**B**) Mechanical unfolding approach using AFM. A single membrane protein in a supported lipid bilayer is partially unfolded to an unstructured polypeptide by vertically pulling the attached AFM tip (left). The partially unfolded protein, with the last helical hairpin still embedded in the bilayer, is refolded by lowering the tip to the membrane surface within 5–10 nm and waiting for up to tens of seconds with the tension relaxed (right). The gray bar at the bottom represents the mica surface supporting the lipid bilayer. (**C**) Mechanical unfolding approach using magnetic tweezers. After unfolding at a high force of tens of pN, the inserted helical state within the lipid bilayer of bicelles is induced by lowering down to a low force of 5–12 pN (left). Refolding of the protein is driven by maintaining the low force for tens of seconds to hours. The mean dwell times at one state before transitioning to another state are measured at different forces and then extrapolated to zero force using force-dependent kinetic models. The serial arrows indicate possible sequential folding transitions to the native folds through intermediate states. Lipid bilayers are shown as sky blue. AFM, atomic force microscopy; SDS, sodium dodecyl sulfate.

The chemical denaturants themselves can impact the folding kinetics by preferentially binding to specific protein sites and altering the solvent space reconstituted for membrane proteins [2,6,57]. The smaller size of mixed detergent/lipid micelles was shown to enhance the folding rates, possibly by constraining the conformational search space during folding [58]. Additionally, the global properties of lipid bilayers can influence the folding speeds as well as the stability of native folds and denatured state ensembles [34,59–61]. For example, an increase in lateral chain pressure has been suggested to slow the formation rates of folding intermediates of bR from SDS-denatured states [34–37]. A recent magnetic tweezer study also indicates that the high viscosity of lipid bilayers significantly retards the helix packing interactions [32], likely serving as a physical origin for the chain pressure effect (see the section *Folding speed limit of helical membrane proteins* for more details).

Employing fluorescence resonance energy transfer (FRET) as a spectroscopic ruler [62,63], Krainer *et al.* observed remarkably rapid folding within time scales of 35–670 μs for a membrane-associating protein Mistic in various detergent micelles [63]. This process initiated from the urea-denatured state with partial helical content. While the ultrafast folding of Mistic is intriguing, its underlying mechanism may not be relevant to helix packing interactions within the membrane mimetics, as the protein is more likely to interact with the membrane surfaces [64]. The absence of characteristic signals representing the correct folding in this approach also raises a question about how non-native states with close contacts can be excluded when assigning the native state.

Table 1. Folding time scales of helical membrane proteins[1]

Protein	Folding transition	Time scale	Membrane mimetics	Method
GlpG	Speed limit of helical hairpin formation within lipid bilayers	~20 ms	DMPC/CHAPSO bicelles	MT [32][2]
	Helical hairpin formation and additional packing within lipid bilayers	110–140 ms	DMPC(70)/DMPG(30)/CHAPSO bicelles[3]	MT [21]
	Folding from unfolded state with full helical content within lipid bilayers	~3 s	DMPC(70)/DMPG(30)/CHAPSO bicelles[3]	MT [21][4]
		~14 s	DMPC(90)/DMPG(10)/CHAPSO bicelles[3]	MT [21][4]
		25–30 s	DMPC/CHAPSO bicelles	MT [21,39][4]
	Folding from unfolded state with full helical content in detergent micelles	~5 s	DDM micelles	SDS + Trp fluorescence [40]
bR	Folding from unfolded state with partial helical content in mixed micelles	3–5 s ~7 s	Mixed DMPC/CHAPS micelles Mixed DMPC/CHAPSO micelles	SDS + absorbance [45] SDS + pulse proteolysis [46]
DsbB	Folding from unfolded state with partial helical content in detergent micelles	1–4 s	DM micelles	SDS + Trp fluorescence [47]

[1]This table presents the time scales extrapolated to zero force or zero denaturant concentration for the designated folding transitions primarily involved in the second-stage folding process;
[2]MT stands for magnetic tweezers. For the other abbreviations, refer to the Abbreviations due to space constraints;
[3]The numbers in parentheses represent the percentage of total lipids (mol%);
[4]The folding time scales are derived from the folded fraction as a function of force using an analysis developed in [39].

Folding speeds under mechanical unfolding approaches

Single-molecule force spectroscopy (SMFS) can more precisely determine the structural states during unfolding or refolding by analyzing molecular extension with force-dependent polymer models [6]. Mechanical force as a denaturant is also decoupled from the chemical forces driving folding and possible chemical disruption of lipid bilayers [2,6]. In atomic force microscopy (AFM)-based SMFS (Figure 2B), a single membrane protein in a supported lipid bilayer is partially unfolded to an unstructured polypeptide by vertically pulling the attached AFM tip. The partially unfolded protein, with the last helical hairpin still embedded in the bilayer, is refolded by lowering the tip to the membrane surface within 5–10 nm and then waiting for up to tens of seconds with the tension relaxed. For the Na^+/H^+ antiporter NhaA, the preferred folding unit of a helical hairpin was observed to refold in a time scale of 1–3 s, estimated as the mean waiting time [65]. A helical segment containing the Na^+-binding site showed a much faster folding rate of ~20 ms. A high-speed AFM probed the rapid refolding transitions of three-residue segments of bR with tens of μs under high force conditions at ~100 pN [66]. In these AFM approaches, the measured time scales are relevant to the spontaneous insertion of unstructured polypeptide portions coupled with helix formation and packing onto the remaining structured template [6,50]. The biased vertical pulling at only one end of the N- or C-terminus introduces variations in refolding pathways and overall folding time scales. The C-terminal pulling design is considered a better mimic of the native insertion and folding process [6].

In single-molecule magnetic tweezers (Figure 2C), the force is applied laterally along the membrane surface at both the N- and C-terminal ends, thereby excluding the potential effect of the biased vertical pulling geometry in AFM. The applied force can remain nearly constant during refolding due to an extremely small spring constant ($k = \Delta F/\Delta z \propto \Delta F \ll 1$), even in a low force range of a few to tens of pN [6]. These inherent system properties enable the capture of the unfolded helical state, where the helices adopt a zigzag configuration within a lipid bilayer at 5–12 pN [21,32]. With this structural state, our focus can be primarily directed towards the helix packing interactions uncoupled from the initial insertion events during refolding, although the helices would not fully traverse the lipid bilayer to the opposite side.

To estimate folding speeds using the tweezer method, mean dwell times at a particular state before transitioning to another state were measured under various forces and then extrapolated to zero force using force-dependent kinetic models. GlpG was shown to predominantly fold in a helical hairpin unit within a bicelle

Biochemical Society Transactions (2024) **52** 491–501
https://doi.org/10.1042/BST20231315

lipid bilayer, exhibiting a time scale of 110–140 ms for each transition [21] (Table 1 and Figure 3A). Despite the applied low force level of 5–7 pN, potential errors in the estimated kinetics may arise from the narrow force window of only 3 pN. Moreover, during the helix packing interactions, the helices effectively rotate within the membrane and the soluble parts fully cross the membrane, possibly influencing the relevant kinetics [32].

The entire folding time of GlpG is notably slower than the intermediate packing transitions, extending to ~3 s [21,39] (Table 1). The large difference in time scales implies repetitive occurrences of formation and dissociation of transient intermediate structures before the final transition to the stable native fold (Figure 3A). Indeed, time-resolved extension traces of GlpG in the low force range demonstrated the frequent, conformational dynamics that eventually disappeared once the protein correctly folded [21]. Based on dissociation time scales, the first intermediate structure of the N-terminal helical hairpin (I_1) would dissociate five times more

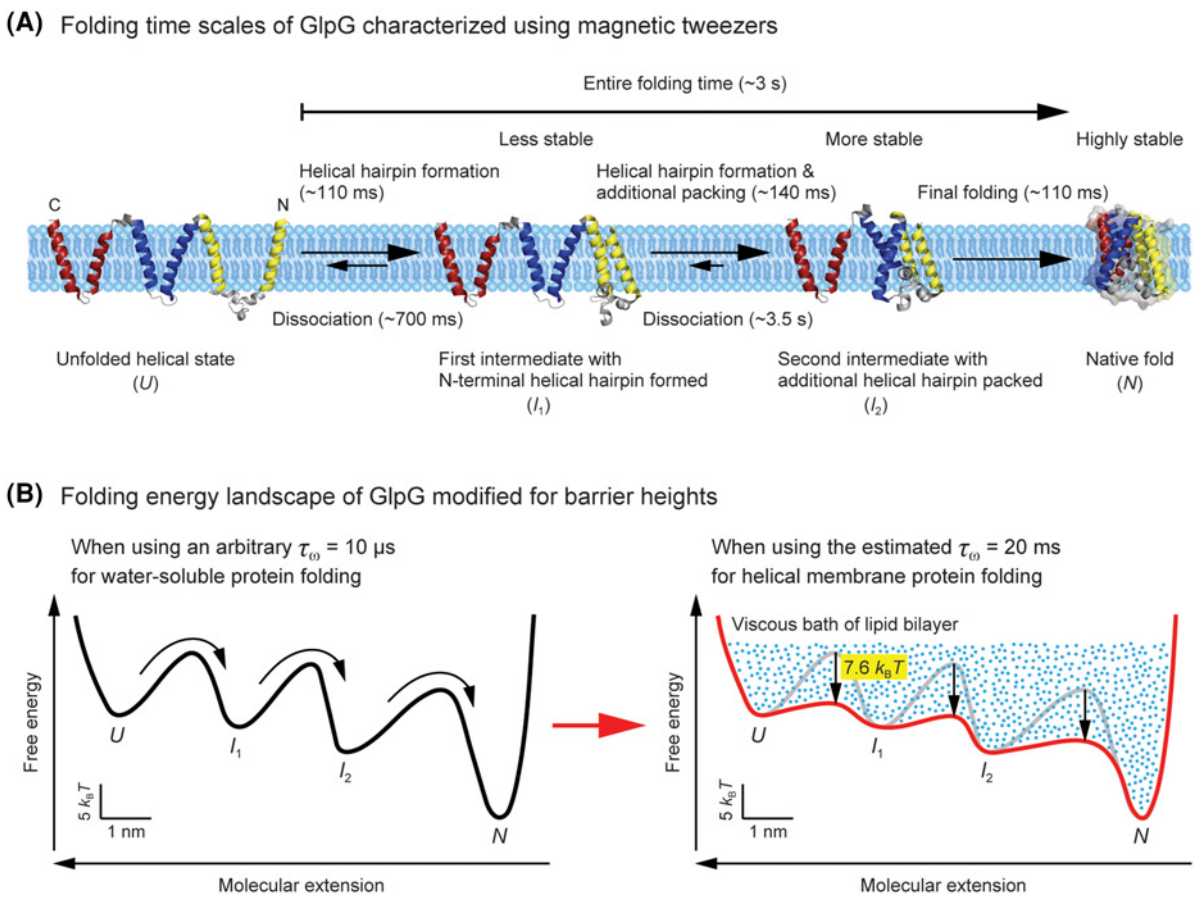

Figure 3. Folding time scales and modified folding energy landscape of GlpG.

(**A**) Folding time scales of GlpG at zero force characterized using magnetic tweezers [21]. The lipid bilayer of bicelles is composed of DMPC and DMPG lipids with a molar ratio of 7 : 3 (depicted in sky blue). In case of the entire folding time, the time scale is derived from the folded fraction as a function of force using an analysis developed in [39]. (**B**) Folding energy landscape of GlpG modified for barrier heights. The energy barrier heights are corrected by the recently estimated τ_ω time scale for the folding speed limit of helical membrane proteins [32]. The left panel shows a reconstructed folding energy landscape of GlpG within the lipid bilayer of DMPC/DMPG bicelles (7:3 mol%) using an arbitrary τ_ω for soluble protein folding [21] (black line), while the right panel shows the modified one for energy barrier heights using the τ_ω estimate for helical membrane proteins [32] (red line). The energy landscape of the left panel is also shown in the right panel as a gray line for comparison. The sky-blue particles depict the high viscosity of lipid bilayers that retards the folding transitions. In the barrier height correction, it is assumed that the membrane viscosity in DMPC bicelles and the resultant τ_ω estimate are not substantially altered in DMPC/DMPG bicelles (7:3 mol%), since DMPG has the same acyl chain and similar bilayer-forming tendency as DMPC [60,61,67]. DMPC, 1,2-dimyristoyl-sn-glycero-3-phosphocholine; DMPG, 1,2-dimyristoyl-sn-glycero-3-phosphorylglycerol.

frequently than the second intermediate structure with two helical hairpins packed (I_2). Especially, the dissociation time scale of I_2 (~3.5 s) is comparable to the entire folding time scale (~3 s), suggesting that once the I_2 state is formed, it serves as a template for packing the last C-terminal helical hairpin (Figure 3A). However, the reverse transition from I_2 to I_1 is still much faster than the translation and insertion, supporting a possibility that the case of transiently assembled folding is more plausible for GlpG among the three possible folding scenarios (Figure 1C). Furthermore, adjusting the lipid composition from DMPC:DMPG = 70:30 mol% to 100 mol % DMPC resulted in an ~10-fold increase in the entire folding time of GlpG [21,39] (Table 1). Although the alteration in lipid head group may primarily impact the folding of soluble and interface parts, the exact mechanism of the retardation remains uncertain.

Modulation of folding speeds by Oxa1 superfamily insertases

It has been consistently observed that large transporters with two TM domains, such as LacY, melibiose permease (MelB), and glucose transporter 3 (GLUT3), are prone to misfolding and/or poor folding in the absence of Oxa1 superfamily insertases [7]. There are hardly any systematic studies examining how the insertases modulate the folding speeds of helical membrane proteins. In studies using AFM, LacY and MelB showed increased overall yields of coupled insertion and folding in the presence of the YidC insertase [68,69]. Yet, it is unclear whether the increased yields with YidC arise from the acceleration of the insertion and folding, prevention of trapping in misfolded states, or a combination of both factors. Likewise, in a study using magnetic tweezers, the folding yield of GLUT3 significantly increased with another Oxa1 superfamily member, the ER membrane protein complex (EMC), in conjunction with phosphatidylethanolamine (PE) lipids [8]. The first passage time from the unfolded state to the fourth intermediate state decreased as the concentration of EMC increased, suggesting that the insertase expedited relevant transitions. However, it is not clear which event was more predominantly affected by EMC during the transitions, such as the helix rotation, soluble part crossing, and helix packing, which were described in the previous section.

Folding speed limit of helical membrane proteins

The so-called folding speed limit has been extensively explored for water-soluble proteins, ranging roughly from 1 μs to 1 ms [70], whereas only recently has it been studied for membrane protein folding [32]. In the Kramers rate framework, represented as $\tau_{folding} = \tau_{\omega} \cdot \exp(\Delta G^{\dagger}/k_B T)$ [71,72], the pre-exponential factor (τ_{ω}) offers a rough estimate of the fastest possible folding time, serving as the upper limit of protein folding speeds [70,73]. Recently developed magnetic tweezers with highly stable molecular tethering have estimated a τ_{ω} value for helical membrane proteins, corresponding to their folding speed limit [32].

Using the robust tweezer method, Kim *et al.* probed persistent transitions between four structural states of a designer four-TM helical bundle (scTMHC2) over an extended 9-h period at a constant force [32]. From the observation of numerous transitions, the authors independently characterized the energy barrier heights ($\Delta G^{\dagger}$) and the folding times ($\tau_{folding}$) between the structural states, while correcting for possible instrumental and molecular system errors. The application of the Kramers formula yielded a τ_{ω} time scale of ~20 ms for the preferred folding unit of a helical hairpin, representing the speed limit of helical hairpin formation within the lipid bilayer of DMPC bicelles [32] (Table 1). As described in the following paragraph, the 20-ms time scale would likely be applicable to other helical hairpins with different residue sequences. It may also be regarded as an estimate for the folding speed limit of entire helical membrane proteome under the specific membrane mimetics.

The estimated time scale of ~20 ms corresponds to an exceedingly slow range compared with that of soluble proteins of similar size by a factor of ~10^4 [32,70], likely attributable to the highly viscous nature of lipid bilayers [32]. Since solvent friction is expected to be the primary determinant for τ_{ω} in the highly viscous medium [74], the speed limit estimation would be less sensitive to residue sequences, although slight sequence-dependent modulations may exist. Additionally, a helical hairpin serves as the minimal folding unit for the tertiary structures of helical membrane proteins [2,20,62]. Larger proteins will thus fold through the packing of additional helical segments onto the initial structural template [2,8,21], taking longer times for complete folding. The helical hairpin formation and additional packing interactions are not physically distinct processes that both occur within lipid bilayers. Lastly, the earlier events of translation and insertion and the other delaying factors as mentioned above can further impede the overall folding process.

Biochemical Society Transactions (2024) **52** 491–501
https://doi.org/10.1042/BST20231315

The same time scale is also applicable to the speed limit of the reverse unfolding transitions, as a similar τ_ω value of ~20 ms was obtained for helical harpin dissociation [32]. The viscosity of the DMPC bicelles and the resultant speed limit estimates would not be substantially altered for other lipids with the same acyl chain and similar bilayer-forming tendency, such as DMPG [60,61,67]. It should be noted, however, that other membrane mimetics and lipid compositions with different viscosity levels may non-negligibly change the speed limit time scales.

Refined architecture of folding energy landscapes

The prior simplistic application of a speed limit range for soluble protein folding likely led to an overestimation of the energy barrier heights associated with (un)folding in helical membrane proteins [21,39,75]. For instance, an energy landscape reconstruction for the second-stage folding of GlpG revealed three transition states with substantial barriers between four structural states [21] (Figure 3B). Each transition primarily involves the formation or dissociation of a helical hairpin (Figure 3A). By adopting the more accurate value of 20 ms for the speed limit time scale, specifically estimated for helical membrane proteins [32], the barrier heights of the transition states are significantly reduced by ~7.6 k_BT (Figure 3C). Consequently, the previously recorded folding times for helical membrane proteins belie the architecture of relevant free energy landscapes. The folding of GlpG within intact lipid bilayers is mostly much slower compared with soluble protein folding (Table 1 and [76]). As mentioned earlier, this sluggish folding process is thought to mainly result from the high membrane viscosity retarding the helix packing interactions, rather than the presence of high energy barriers and/or ruggedness over the barriers. It still remains uncertain, however, whether the refined folding energy landscape is maintained, even during the co-translational folding involving the ribosome–translocon complex.

Perspectives

- Membrane protein folding is a fundamental biophysical problem that needs to be addressed to enhance the treatment of conformational disorders arising from misfolding. While unraveling the kinetic details is crucial for a comprehensive mechanistic understanding, only a limited body of research is available for helical membrane proteins, mainly due to technical limitations across various facets.

- The folding speeds of helical membrane proteins are primarily limited by the earlier steps of translation and insertion but can be substantially delayed by other factors, such as strong packing cooperativity and post-insertion topology changes. The viscosity of lipid membranes emerges as a notable factor that decelerates helix packing interactions, significantly altering the current picture of folding energy landscapes.

- A promising direction for future research involves mechanistic studies aimed at understanding how the precise timing of insertion and folding steps coordinates the entire co-translational folding process while mitigating the risks of misfolding and aggregation. An essential question in this context pertains to when and where insertases and chaperones participate in the folding process and how they contribute to reorganizing the sequence and timing of intermediate steps.

Competing Interests

The author declares that there are no competing interests associated with this manuscript.

Funding

This work was supported and funded by the National Research Foundation of Korea [2020R1C1C1003937].

Acknowledgements

The author thanks Seoyoon Kim in his laboratory for help with preparing a figure.

Abbreviations

AFM, atomic force microscopy; bR, bacteriorhodopsin; CHAPS, 3-[(3-cholamidopropyl) dimethylammonio]-1-propanesulfonate; CHAPSO, 3-[(3-cholamidopropyl) dimethylammonio]-2-hydroxy-1-propanesulfonate; DDM, *n*-dodecyl β-D-maltoside; DM, *n*-decyl β-D-maltoside; DMPC, 1,2-dimyristoyl-sn-glycero-3-phosphocholine; DMPG, 1,2-dimyristoyl-sn-glycero-3-phosphorylglycerol; DsbB, disulfide bond formation protein B; EMC, endoplasmic reticulum membrane protein complex; ER, endoplasmic reticulum; FRET, fluorescence resonance energy transfer; GLUT3, glucose transporter 3; LacY, lactose permease; MelB, melibiose permease; MT, magnetic tweezers; PE, phosphatidylethanolamine; PMP22, peripheral myelin protein 22; SDS, sodium dodecyl sulfate; SEIRAS, surface-enhanced infrared absorption spectroscopy; SMFS, single-molecule force spectroscopy; TM, transmembrane; Trp, tryptophan.

References

1 Hegde, R.S. and Keenan, R.J. (2022) The mechanisms of integral membrane protein biogenesis. *Nat. Rev. Mol. Cell Biol.* **23**, 107–124 https://doi.org/10.1038/s41580-021-00413-2
2 Corin, K. and Bowie, J.U. (2022) How physical forces drive the process of helical membrane protein folding. *EMBO Rep.* **23**, e53025 https://doi.org/10.15252/embr.202153025
3 Mercier, E., Wang, X., Bogeholz, L.A.K., Wintermeyer, W. and Rodnina, M.V. (2022) Cotranslational biogenesis of membrane proteins in bacteria. *Front. Mol. Biosci.* **9**, 871121 https://doi.org/10.3389/fmolb.2022.871121
4 Cymer, F., von Heijne, G. and White, S.H. (2015) Mechanisms of integral membrane protein insertion and folding. *J. Mol. Biol.* **427**, 999–1022 https://doi.org/10.1016/j.jmb.2014.09.014
5 Shao, S.C. and Hegde, R.S. (2011) Membrane protein insertion at the endoplasmic reticulum. *Annu. Rev. Cell Dev. Biol.* **27**, 25–56 https://doi.org/10.1146/annurev-cellbio-092910-154125
6 Wijesinghe, W.C.B. and Min, D.Y. (2023) Single-molecule force spectroscopy of membrane protein folding. *J. Mol. Biol.* **435**, 167975 https://doi.org/10.1016/j.jmb.2023.167975
7 Kim, E. and Min, D. (2023) Chaperoning the major facilitator superfamily at single-molecule level. *Structure* **31**, 1291–1294 https://doi.org/10.1016/j.str.2023.10.003
8 Choi, H.K., Kang, H., Lee, C., Kim, H.G., Phillips, B., Park, S. et al. (2022) Evolutionary balance between foldability and functionality of a glucose transporter. *Nat. Chem. Biol.* **18**, 713 https://doi.org/10.1038/s41589-022-01002-w
9 Min, D., Jefferson, R.E., Qi, Y., Wang, J.Y., Arbing, M.A., Im, W. et al. (2018) Unfolding of a ClC chloride transporter retains memory of its evolutionary history. *Nat. Chem. Biol.* **14**, 489–496 https://doi.org/10.1038/s41589-018-0025-4
10 Marinko, J.T., Huang, H., Penn, W.D., Capra, J.A., Schlebach, J.P. and Sanders, C.R. (2019) Folding and misfolding of human membrane proteins in health and disease: from single molecules to cellular proteostasis. *Chem. Rev.* **119**, 5537–5606 https://doi.org/10.1021/acs.chemrev.8b00532
11 Matamouros, S., Gensch, T., Cerff, M., Sachs, C.C., Abdollahzadeh, I., Hendriks, J. et al. (2023) Growth-rate dependency of ribosome abundance and translation elongation rate in *Corynebacterium glutamicum* differs from that in *Escherichia coli*. *Nat. Commun.* **14**, 5611 https://doi.org/10.1038/s41467-023-41176-y
12 Gerashchenko, M.V., Peterfi, Z., Yim, S.H. and Gladyshev, V.N. (2021) Translation elongation rate varies among organs and decreases with age. *Nucleic Acids Res.* **49**, e9 https://doi.org/10.1093/nar/gkaa1103
13 Mercier, E., Wintermeyer, W. and Rodnina, M.V. (2020) Co-translational insertion and topogenesis of bacterial membrane proteins monitored in real time. *EMBO J.* **39**, e104054 https://doi.org/10.15252/embj.2019104054
14 Hershey, J.W.B., Sonenberg, N. and Mathews, M.B. (2019) Principles of translational control. *Cold Spring Harb. Perspect. Biol.* **11**, a032607 https://doi.org/10.1101/cshperspect.a032607
15 Riba, A., Di Nanni, N., Mittal, N., Arhne, E., Schmidt, A. and Zavolan, M. (2019) Protein synthesis rates and ribosome occupancies reveal determinants of translation elongation rates. *Proc. Natl Acad. Sci. U.S.A.* **116**, 15023–15032 https://doi.org/10.1073/pnas.1817299116
16 Zhu, M.L. and Dai, X.F. (2019) Maintenance of translational elongation rate underlies the survival of *Escherichia coli* during oxidative stress. *Nucleic Acids Res.* **47**, 7592–7604 https://doi.org/10.1093/nar/gkz467
17 Wu, B., Eliscovich, C., Yoon, Y.J. and Singer, R.H. (2016) Translation dynamics of single mRNAs in live cells and neurons. *Science* **352**, 1430–1435 https://doi.org/10.1126/science.aaf1084
18 Hershey, J.W.B. (1991) Translational control in mammalian-cells. *Annu. Rev. Biochem.* **60**, 717–755 https://doi.org/10.1146/annurev.bi.60.070191.003441
19 Dale, H. and Krebs, M.P. (1999) Membrane insertion kinetics of a protein domain in vivo. The bacterioopsin n terminus inserts co-translationally. *J. Biol. Chem.* **274**, 22693–22698 https://doi.org/10.1074/jbc.274.32.22693
20 Engelman, D.M. and Steitz, T.A. (1981) The spontaneous insertion of proteins into and across membranes - the helical hairpin hypothesis. *Cell* **23**, 411–422 https://doi.org/10.1016/0092-8674(81)90136-7
21 Choi, H.K., Min, D., Kang, H., Shon, M.J., Rah, S.H., Kim, H.C. et al. (2019) Watching helical membrane proteins fold reveals a common N-to-C-terminal folding pathway. *Science* **366**, 1150–1156 https://doi.org/10.1126/science.aaw8208
22 Vitrac, H., Mallampalli, V.K.P.S., Bogdanov, M. and Dowhan, W. (2019) The lipid-dependent structure and function of LacY can be recapitulated and analyzed in phospholipid-containing detergent micelles. *Sci. Rep.* **9**, 11338 https://doi.org/10.1038/s41598-019-47824-y
23 Seurig, M., Ek, M., von Heijne, G. and Fluman, N. (2019) Dynamic membrane topology in an unassembled membrane protein. *Nat. Chem. Biol.* **15**, 945–948 https://doi.org/10.1038/s41589-019-0356-9
24 Woodall, N.B., Hadley, S., Yin, Y. and Bowie, J.U. (2017) Complete topology inversion can be part of normal membrane protein biogenesis. *Protein Sci.* **26**, 824–833 https://doi.org/10.1002/pro.3131

Biochemical Society Transactions (2024) **52** 491–501
https://doi.org/10.1042/BST20231315

25 Vitrac, H., MacLean, D.M., Jayaraman, V., Bogdanov, M. and Dowhan, W. (2015) Dynamic membrane protein topological switching upon changes in phospholipid environment. *Proc. Natl Acad. Sci. U.S.A.* **112**, 13874–13879 https://doi.org/10.1073/pnas.1512994112

26 Dowhan, W. and Bogdanov, M. (2011) Lipid-protein interactions as determinants of membrane protein structure and function. *Biochem. Soc. Trans.* **39**, 767–774 https://doi.org/10.1042/Bst0390767

27 Lu, Y., Turnbull, I.R., Bragin, A., Carveth, K., Verkman, A.S. and Skach, W.R. (2000) Reorientation of aquaporin-1 topology during maturation in the endoplasmic reticulum. *Mol. Biol. Cell* **11**, 2973–2985 https://doi.org/10.1091/mbc.11.9.2973

28 Schafer, N.P., Truong, H.H., Otzen, D.E., Lindorff-Larsen, K. and Wolynes, P.G. (2016) Topological constraints and modular structure in the folding and functional motions of GlpG, an intramembrane protease. *Proc. Natl Acad. Sci. U.S.A.* **113**, 2098–2103 https://doi.org/10.1073/pnas.1524027113

29 Baumann, A., Kerruth, S., Fitter, J., Buldt, G., Heberle, J., Schlesinger, R. et al. (2016) In-situ observation of membrane protein folding during cell-free expression. *PLoS One* **11**, e0151051 https://doi.org/10.1371/journal.pone.0151051

30 Booth, P.J. (2000) Unravelling the folding of bacteriorhodopsin. *Biochim. Biophys. Acta* **1460**, 4–14 https://doi.org/10.1016/s0005-2728(00)00125-0

31 Booth, P.J., Flitsch, S.L., Stern, L.J., Greenhalgh, D.A., Kim, P.S. and Khorana, H.G. (1995) Intermediates in the folding of the membrane protein bacteriorhodopsin. *Nat. Struct. Biol.* **2**, 139–143 https://doi.org/10.1038/nsb0295-139

32 Kim, S., Lee, D., Wijesinghe, W.C.B. and Min, D. (2023) Robust membrane protein tweezers reveal the folding speed limit of helical membrane proteins. *Elife* **12**, e85882 https://doi.org/10.7554/eLife.85882

33 Muhammednazaar, S., Yao, J., Guo, R., Rhee, M.S., Kim, K.H., Kang, S.-G. et al. (2023) Lipid bilayer strengthens the cooperative network of a membrane-integral enzyme. *bioRxiv* 2023.2005.2030.542905 https://doi.org/10.1101/2023.05.30.542905

34 Booth, P.J. (2005) Sane in the membrane: designing systems to modulate membrane proteins. *Curr. Opin. Struct. Biol.* **15**, 435–440 https://doi.org/10.1016/j.sbi.2005.06.002

35 Allen, S.J., Curran, A.R., Templer, R.H., Meijberg, W. and Booth, P.J. (2004) Folding kinetics of an alpha helical membrane protein in phospholipid bilayer vesicles. *J. Mol. Biol.* **342**, 1279–1291 https://doi.org/10.1016/j.jmb.2004.07.040

36 Allen, S.J., Curran, A.R., Templer, R.H., Meijberg, W. and Booth, P.J. (2004) Controlling the folding efficiency of an integral membrane protein. *J. Mol. Biol.* **342**, 1293–1304 https://doi.org/10.1016/j.jmb.2004.07.041

37 Booth, P.J., Riley, M.L., Flitsch, S.L., Templer, R.H., Farooq, A., Curran, A.R. et al. (1997) Evidence that bilayer bending rigidity affects membrane protein folding. *Biochemistry* **36**, 197–203 https://doi.org/10.1021/bi962200m

38 Guo, R., Gaffney, K., Yang, Z., Kim, M., Sungsuwan, S., Huang, X. et al. (2016) Steric trapping reveals a cooperativity network in the intramembrane protease GlpG. *Nat. Chem. Biol.* **12**, 353–360 https://doi.org/10.1038/nchembio.2048

39 Min, D., Jefferson, R.E., Bowie, J.U. and Yoon, T.Y. (2015) Mapping the energy landscape for second-stage folding of a single membrane protein. *Nat. Chem. Biol.* **11**, 981–987 https://doi.org/10.1038/nchembio.1939

40 Paslawski, W., Lillelund, O.K., Kristensen, J.V., Schafer, N.P., Baker, R.P., Urban, S. et al. (2015) Cooperative folding of a polytopic alpha-helical membrane protein involves a compact N-terminal nucleus and nonnative loops. *Proc. Natl Acad. Sci. U.S.A.* **112**, 7978–7983 https://doi.org/10.1073/pnas.1424751112

41 Schlebach, J.P., Peng, D., Kroncke, B.M., Mittendorf, K.F., Narayan, M., Carter, B.D. et al. (2013) Reversible folding of human peripheral myelin protein 22, a tetraspan membrane protein. *Biochemistry* **52**, 3229–3241 https://doi.org/10.1021/bi301635f

42 Myers, J.K., Mobley, C.K. and Sanders, C.R. (2008) The peripheral neuropathy-linked Trembler and Trembler-J mutant forms of peripheral myelin protein 22 are folding-destabilized. *Biochemistry* **47**, 10620–10629 https://doi.org/10.1021/bi801157p

43 Popot, J.L. and Engelman, D.M. (1990) Membrane protein folding and oligomerization: the two-stage model. *Biochemistry* **29**, 4031–4037 https://doi.org/10.1021/bi00469a001

44 Engelman, D.M., Chen, Y., Chin, C.N., Curran, A.R., Dixon, A.M., Dupuy, A.D. et al. (2003) Membrane protein folding: beyond the two stage model. *FEBS Lett.* **555**, 122–125 https://doi.org/10.1016/s0014-5793(03)01106-2

45 Curnow, P. and Booth, P.J. (2007) Combined kinetic and thermodynamic analysis of alpha-helical membrane protein unfolding. *Proc. Natl Acad. Sci. U.S.A.* **104**, 18970–18975 https://doi.org/10.1073/pnas.0705067104

46 Schlebach, J.P., Cao, Z., Bowie, J.U. and Park, C. (2012) Revisiting the folding kinetics of bacteriorhodopsin. *Protein Sci.* **21**, 97–106 https://doi.org/10.1002/pro.766

47 Otzen, D.E. (2003) Folding of DsbB in mixed micelles: a kinetic analysis of the stability of a bacterial membrane protein. *J. Mol. Biol.* **330**, 641–649 https://doi.org/10.1016/s0022-2836(03)00624-7

48 Harris, N.J., Pellowe, G.A., Blackholly, L.R., Gulaidi-Breen, S., Findlay, H.E. and Booth, P.J. (2022) Methods to study folding of alpha-helical membrane proteins in lipids. *Open Biol.* **12**, 220054 https://doi.org/10.1098/rsob.220054

49 Pellowe, G.A. and Booth, P.J. (2020) Structural insight into co-translational membrane protein folding. *Biochim. Biophys. Acta Biomembr.* **1862**, 183019 https://doi.org/10.1016/j.bbamem.2019.07.007

50 Jefferson, R.E., Min, D., Corin, K., Wang, J.Y. and Bowie, J.U. (2018) Applications of single-molecule methods to membrane protein folding studies. *J. Mol. Biol.* **430**, 424–437 https://doi.org/10.1016/j.jmb.2017.05.021

51 Harris, N.J., Reading, E., Ataka, K., Grzegorzewski, L., Charalambous, K., Liu, X. et al. (2017) Structure formation during translocon-unassisted co-translational membrane protein folding. *Sci. Rep.* **7**, 8021 https://doi.org/10.1038/s41598-017-08522-9

52 Booth, P.J. (2012) A successful change of circumstance: a transition state for membrane protein folding. *Curr. Opin. Struct. Biol.* **22**, 469–475 https://doi.org/10.1016/j.sbi.2012.03.008

53 Booth, P.J. and Curnow, P. (2006) Membrane proteins shape up: understanding in vitro folding. *Curr. Opin. Struct. Biol.* **16**, 480–488 https://doi.org/10.1016/j.sbi.2006.06.004

54 Mackenzie, K.R. (2006) Folding and stability of alpha-helical integral membrane proteins. *Chem. Rev.* **106**, 1931–1977 https://doi.org/10.1021/cr0404388

55 Booth, P.J. (1997) Folding alpha-helical membrane proteins: kinetic studies on bacteriorhodopsin. *Fold Des.* **2**, R85–R92 https://doi.org/10.1016/s1359-0278(97)00045-x

56 Chang, Y.C. and Bowie, J.U. (2014) Measuring membrane protein stability under native conditions. *Proc. Natl Acad. Sci. U.S.A.* **111**, 219–224 https://doi.org/10.1073/pnas.1318576111

57 Otzen, D.E., Pedersen, J.N., Somavarapu, A.K., Clement, A., Ji, M., Petersen, E.H. et al. (2021) Cys-labeling kinetics of membrane protein GlpG: a role for specific SDS binding and micelle changes? *Biophys. J.* **120**, 4115–4128 https://doi.org/10.1016/j.bpj.2021.08.001
58 Gruenhagen, T.C., Ziarek, J.J. and Schlebach, J.P. (2018) Bicelle size modulates the rate of bacteriorhodopsin folding. *Protein Sci.* **27**, 1109–1112 https://doi.org/10.1002/pro.3414
59 Gaffney, K.A., Guo, R., Bridges, M.D., Muhammednazaar, S., Chen, D., Kim, M. et al. (2022) Lipid bilayer induces contraction of the denatured state ensemble of a helical-bundle membrane protein. *Proc. Natl Acad. Sci. U.S.A.* **119**, e2109169119 https://doi.org/10.1073/pnas.2109169119
60 Brady, R., Harris, N.J., Pellowe, G.A., Breen, S.G. and Booth, P.J. (2022) How lipids affect the energetics of co-translational alpha helical membrane protein folding. *Biochem. Soc. Trans.* **50**, 555–567 https://doi.org/10.1042/Bst20201063
61 Corin, K. and Bowie, J.U. (2020) How bilayer properties influence membrane protein folding. *Protein Sci.* **29**, 2348–2362 https://doi.org/10.1002/pro.3973
62 Krainer, G., Treff, A., Hartmann, A., Stone, T.A., Schenkel, M., Keller, S. et al. (2018) A minimal helical-hairpin motif provides molecular-level insights into misfolding and pharmacological rescue of CFTR. *Commun. Biol.* **1**, 154 https://doi.org/10.1038/s42003-018-0153-0
63 Krainer, G., Hartmann, A., Anandamurugan, A., Gracia, P., Keller, S. and Schlierf, M. (2018) Ultrafast protein folding in membrane-mimetic environments. *J. Mol. Biol.* **430**, 554–564 https://doi.org/10.1016/j.jmb.2017.10.031
64 Marino, J., Bordag, N., Keller, S. and Zerbe, O. (2015) Mistic's membrane association and its assistance in overexpression of a human GPCR are independent processes. *Protein Sci.* **24**, 38–48 https://doi.org/10.1002/pro.2582
65 Kedrov, A., Janovjak, H., Ziegler, C., Kuhlbrandt, W. and Muller, D.J. (2006) Observing folding pathways and kinetics of a single sodium-proton antiporter from *Escherichia coli*. *J. Mol. Biol.* **355**, 2–8 https://doi.org/10.1016/j.jmb.2005.10.028
66 Yu, H., Siewny, M.G., Edwards, D.T., Sanders, A.W. and Perkins, T.T. (2017) Hidden dynamics in the unfolding of individual bacteriorhodopsin proteins. *Science* **355**, 945–950 https://doi.org/10.1126/science.aah7124
67 Renne, M.F. and Ernst, R. (2023) Membrane homeostasis beyond fluidity: control of membrane compressibility. *Trends Biochem. Sci.* **48**, 963–977 https://doi.org/10.1016/j.tibs.2023.08.004
68 Blaimschein, N., Parameswaran, H., Nagler, G., Manioglu, S., Helenius, J., Ardelean, C. et al. (2023) The insertase YidC chaperones the polytopic membrane protein MelB inserting and folding simultaneously from both termini. *Structure* **31**, 1419–1430.e5 https://doi.org/10.1016/j.str.2023.08.012
69 Serdiuk, T., Balasubramaniam, D., Sugihara, J., Mari, S.A., Kaback, H.R. and Muller, D.J. (2016) Yidc assists the stepwise and stochastic folding of membrane proteins. *Nat. Chem. Biol.* **12**, 911–917 https://doi.org/10.1038/nchembio.2169
70 Kubelka, J., Hofrichter, J. and Eaton, W.A. (2004) The protein folding 'speed limit'. *Curr. Opin. Struct. Biol.* **14**, 76–88 https://doi.org/10.1016/j.sbi.2004.01.013
71 Hanggi, P., Talkner, P. and Borkovec, M. (1990) Reaction-rate theory - 50 years after Kramers. *Rev. Mod. Phys.* **62**, 251–341 https://doi.org/10.1103/revmodphys.62.251
72 Hagen, S.J. (2010) Solvent viscosity and friction in protein folding dynamics. *Curr. Protein Pept. Sci.* **11**, 385–395 https://doi.org/10.2174/138920310791330596
73 Chung, H.S. and Eaton, W.A. (2018) Protein folding transition path times from single molecule FRET. *Curr. Opin. Struct. Biol.* **48**, 30–39 https://doi.org/10.1016/j.sbi.2017.10.007
74 Ansari, A., Jones, C.M., Henry, E.R., Hofrichter, J. and Eaton, W.A. (1992) The role of solvent viscosity in the dynamics of protein conformational-changes. *Science* **256**, 1796–1798 https://doi.org/10.1126/science.1615323
75 Lu, P.L., Min, D.Y., DiMaio, F., Wei, K.Y., Vahey, M.D., Boyken, S.E. et al. (2018) Accurate computational design of multipass transmembrane proteins. *Science* **359**, 1042–1046 https://doi.org/10.1126/science.aaq1739
76 Munoz, V. and Eaton, W.A. (1999) A simple model for calculating the kinetics of protein folding from three-dimensional structures. *Proc. Natl Acad. Sci. U.S.A.* **96**, 11311–11316 https://doi.org/10.1073/pnas.96.20.11311